Remarkable Improvement on the Methane Aromatization Reaction: A Highly Selective and Coking-Resistant Catalyst

Ding Ma,[†] Yuan Lu,[‡] Lingling Su,[†] Zhusheng Xu,[‡] Zhijian Tian,[‡] Yide Xu,[†] Liwu Lin,*[,‡] and Xinhe Bao*[,†]

State Key Laboratory of Catalysis, and Laboratory of Natural Gas Utilization and Applied Catalysis, Dalian Institute of Chemical Physics, The Chinese Academy of Sciences, Dalian 116023, P. R. China

Received: January 17, 2002; In Final Form: April 30, 2002

An effective way (without addition of any oxidative gases to the reactant) to suppress coke formation (by modification of the Mo/HZSM-5 catalyst) and thus to significantly improve the aromatic selectivity in the methane aromatization reaction is presented in this study. A greater yield of benzene and an enhanced durability of the catalyst when compared with the conventional Mo/HZSM-5 catalysts are observed. Multinuclear solid-state NMR, TPD, TPO, TG, and UV−Raman methods are applied to characterize and rationalize the structure−property relationship of the improved catalytic performance of the modified catalysts. From this work, we found that only a small fraction of tetrahedral framework aluminum, which corresponds to the Bronsted acid sites, is sufficient to accomplish the aromatization of the intermediates in methane aromatization reaction, while the superfluous strong Bronsted acid sites, which can be removed upon steaming treatment, are shown to be related with the aromatic carbonaceous deposits on the catalysts.

1. Introduction

Natural gas (mostly methane) reserves are abundant throughout the world and are becoming a promising energy source due to the increasing prices of oil. A major limitation to the utilization of the resource is the high price to transport the natural gas to the desired location.[1] Therefore, one of the current challenges of the petrochemical industry is to develop more economical processes of directly upgrading vast worldwide reserves of natural gas at its source to higher valued liquid fuels and petrochemical intermediates. Normally there are two approaches for the direct selective conversion of methane, namely oxidative and nonoxidative transformations.[2−4] For both the processes, the scission of a C−H bond is the first step that a methane transformation reaction encounters. Due to its perfect symmetry, methane has the most stable C−H bonds when compared with its homologues such as ethane and propane; thus, the activation of the C−H bond of methane needs relatively higher temperature.[2,3] However, the high temperature used aggravates a selective reaction,[5] i.e. for oxidative reactions, a weaker C−H bond of the product with respect to that of the methane results in difficulty in efficiently controlling the degree of oxidation, whereas for other reactions, such as nonoxidative aromatization, suppression of the coke formation during the reaction remains a major problem.

A methane aromatization reaction realized on bifunctional Mo/HZSM-5 catalysts is a typical example of these nonoxidative reactions.[6−14] At 973 K and 1 atm, the formations of aromatics are accompanied by the deposition of about 20−40% of the converted methane on the surface of the catalysts as coke species, thus lowering the selectivity to desired products. At the same time, the coke deposits that gradually accumulated may result in the coverage of the acid sites of the zeolite and will eventually lead to the blockage of the channels/pores of the zeolite, thus making the active sites inaccessible for the reactant and other reaction intermediates. Therefore, a short lifetime is observed for this reaction. With the aim of finding a way to elongate the relatively short lifetime of this reaction, great attention has been paid to the suppression of coke formation for this reaction. Ichikawa et al. reported that through addition of a small amount of CO or CO_2 into the reactant mixture, an improvement of catalyst stability and a better catalytic performance (lower coke selectivity and higher benzene yield) were achieved.[15,16] They suggested that the unique role of CO addition to the methane feed is based on the formation of minute amounts of CO_2 and C by the Boudart reaction, where C is hydrogenated to a common active CH_x species, while CO_2 reacts with the surface inert coke to CO, thus leading to the observed better catalytic performance due to efficient suppression of coke formation on the catalysts.[16] At the same time, the addition of O_2 (up to O_2/CH_4 molar ratios of 5.5×10^{-3} molar ratios) to the reactant has been proven to be similarly efficient in improving the durability.[17] Through UV−Raman experiments, the authors attributed the improved catalyst durability to the removal of part of the coke deposits and keeping the catalyst as MoO_xC_y/HZSM-5. However, using an oxidative cofeed material will inevitably increase the complexity of the reaction requirements and at the same time increase the cost of using this reaction at an industrial level. Thus, there remains a need to find a better method toward the improvement of the catalyst durability. Howe et al. have observed that during the methanol to gasoline (MTG) conversion reaction, the catalyst, HZSM-5, will be dealuminated extensively by water produced in the MTG reaction.[18] Interestingly, the catalyst lifetimes, however, increased after repeated use in MTG cycles. This was attributed to the removal of redundant lattice aluminum. On the other hand, it is well-known that modification of the acidity of zeolite through hydrothermal treatment can be controlled by varying

* Corresponding authors. Telephone: 0086-411-4379116 (office). Fax: 0086-411-4694447. E-mail: xhbao@dicp.ac.cn (X.B.) and linliwu@mail.dlptt.ln.cn (L.L.).

[†] State Key Laboratory of Catalysis.

[‡] Laboratory of Natural Gas Utilization and Applied Catalysis.

10.1021/jp020166h CCC: $22.00
Published on Web 07/25/2002

the steaming temperature, the partial pressure of steam, and the time of the treatment.[19] In light of the above observations, we studied the effect of the steaming dealumination effect on the catalytic performance of Mo/HZSM-5 catalysts for methane aromatization.[20] Dramatic improvements regarding the catalyst performance and durability are achieved from this method, i.e. after 10 h reaction at 1023 K, the benzene yield in a properly dealuminated ZSM-5 supported Mo catalyst increases about 60%, while the selectivity to coke drops significantly from 36 to 18% when compared with the conventional Mo/HZSM-5 catalyst. Furthermore, this work was also investigated using solid-state NMR, TPD, TPO (temperature-programmed oxidation), in situ TG, and UV−Raman spectroscopy to rationalize the structure−property relationship in methane aromatization reaction.

2. Experimental Section

Sample Preparation. HZSM-5 with a Si/Al mole ratio of 25 (denoted as HZSM-5(P), supplied by Nankai University) was used as the parent zeolite. The dealumination of the parent zeolite was realized by a steaming method, resulting in a series of dealuminated samples (HZSM-5(STn), $n = 1-3$). The steam treatment conditions (temperature/K, partial pressure of steam/kPa, time/h) of HZSM-5(ST1), HZSM-5(ST2) and HZSM-5(ST3) were (773, 38, 6), (823, 38, 6) and (823, 70, 6), respectively. With n varying from 1 to 3, the severity of dealumination increases. After the steam treatment, the samples were washed by 0.5 N HCl solution at room temperature in order to remove the additional extraframework aluminum species (which are possibly responsible for part of the coke formation) that were expelled from the zeolite lattice during the steaming. The parent HZSM-5 was treated with 0.5 N HCl prior to Mo loading and denoted as HZSM-5(HCl) for the blank experiment. No obvious dealumination of HZSM-5(HCl) was detected compared with HZSM-5(P). Mo-containing catalysts (Mo wt % = 4%) were prepared by incipient wetness impregnation of HZSM-5(P), HZSM-5(HCl), and HZSM-5(STn) (n = 1, 2, 3) with an aqueous solution of ammonium heptamolybdate ($(NH_4)_6Mo_7O_{24}\cdot H_2O$). After impregnation, the catalysts were dried at 383 K for 4 h and then calcined in air at 823 K for 6 h. The catalysts were crushed and sieved to 40−60 mesh granules for further use.

Catalytic Evaluation. Methane aromatization reactions were carried out in a continuous flow reactor system equipped with a quartz tube (10 mm id) packed with 1.5 mL of catalyst pellets of 40−60 mesh. A feed gas mixture of 97.5% CH_4 with 2.5% Ar was purified and then introduced into the reactor at a flow rate of 1500 mL/g h (GHSV = 600 h^{-1}). The reaction was conducted at 973 and 1023 K under a total pressure of 1 atm. The tail gas out of the reactor was detected on-line by a six-way valve connected with two sets of gas chromatographs. The conversion of methane and selectivity to products including ethylene, ethane, benzene, toluene, naphthalene, CO, and CO_2 are calculated by a method similar to that reported by Liu et al.[11] Details can be found elsewhere.[17]

Solid-State NMR. All the NMR spectra were recorded at 9.4 T on a Bruker DRX-400 spectrometer using 4 mm ZrO_2 rotors. ^{29}Si MAS NMR spectra were recorded at 79.5 MHz using a 0.8 μs ($\pi/8$) pulse with a 4 s recycle delay and 3000 scans. The magic angle spinning rate for all ^{29}Si spectra was 4 kHz, and chemical shifts were referenced to 4,4-dimethyl-4-silapentane sulfonate sodium (DSS). ^{27}Al MAS NMR spectra were recorded at 104.3 MHz using a 0.75 μs ($\pi/12$) pulse with a 3 s recycle delay and 600 scans. 1% aqueous $Al(H_2O)_6^{3+}$ was used as the reference of chemical shifts, and samples were spun at 4 kHz. ^{1}H MAS NMR spectra were collected at 400.1 MHz using single-pulse experiments with $\pi/2$ pulse and a 4 s recycle delay. Prior to the proton NMR measurements, the samples were dehydrated at 673K and 10^{-2} Pa for about 20 h in a homemade apparatus, by which the treated sample can be filled in situ into a NMR rotor, sealed, and transferred to the spectrometer without exposure to air. All the ^{1}H MAS NMR spectra were accumulated for 200 scans and spun at 8 kHz. The chemical shifts were referenced to a saturated aqueous solution of DSS.

NH_3-TPD, Benzene-TPD, and TPO Experiments. For the NH_3-TPD experiment, the sample (0.14 g) was dried in a flowing He (99.99%, 30 mL/min) at 873 K for 0.5 h prior to adsorption. Pure NH_3 was adsorped until saturation took place at 323 K, then the catalyst was flushed with He at the same temperature for 1 h. TPD measurements were conducted from 323 to 900 K with a heating rate of 15 K/min, with He as the carrier gas. The amount of desorbed ammonia was detected by a thermal conductive detector. Benzene-TPD experiments were conducted on a conventional TP-MS apparatus that has been described in elsewhere. Before adsorption, the sample (0.15 g) was heated in a He flow (99.99%, 40 mL/min) at 873 K for 0.5 h to remove the adsorbed water. Then, benzene was adsorbed at 323 K by passing a He stream (40 mL/min) that was saturated with benzene vapor at 273 K over the catalysts. After equilibrium had been reached (about 30 min), the catalyst was flushed with He at the same temperature for 1 h. TPD measurements were done from 323 to 683 K at a linear heating rate of 10 K/min, with He as the carrier gas (40 mL/min). The signal of desorbed benzene was detected by an on-line quadruple mass spectrometer (Balzers, QMS 200). TPO (Temperature programmed oxidation) experiments of coked catalysts (after 8 h time on stream, 1 atm, GHSV = 600 h^{-1}) were performed with a 20% O_2/He mixture (20 mL/min, after dehydration) as the oxidant at a heating rate of 10 K/min. The concentrations of CO_2 in the discharged gas were monitored by gas chromatography.

In Situ TG. The in situ TG measurements were conducted on a Perkin-Elmer TGS-2 instrument. The catalyst charge was 0.03 g, and the identical reaction procedure with the fixed-bed methane aromatization reaction has been taken in TG measurements. The catalyst weight increase during the reaction is detected by the TG method. The coke formation rate is represented by the slope of the specific weight increase curve.

UV−Raman Measurements. UV−Raman spectra were recorded on a homemade spectrometer, which consists of an intracavity frequency-doubled Ar^+ ion laser (Coherent, Innova 300 FRED), using a line at 257 nm as the excitation source, a three-grating spectrometer (Spex Triplemate 1877D), and a CCD detector (EG&G Co., Ltd.). The resolution of the Raman system was about 1.5 cm^{-1} (at 257 nm excitation), and the power of the 257 nm laser line at the sample was kept at about 2 mW to avoid overheating of the sample.

3. Results and Discussion

3.1. Zeolite Characterization. It is well-known that NMR is a suitable tool to measure the structure changes of zeolites. Here multinuclear solid-state NMR is used to characterize the structural changes of the HZSM-5 zeolite before and after hydrothermal treatment. The ^{29}Si MAS NMR spectra of parent HZSM-5 and three steam-dealuminated HZSM-5 zeolites are shown in Figure 1. Three distinct signals at −117, −114 and −108 ppm are clearly resolved in the ^{29}Si NMR of untreated HZSM-5. The two peaks at high field part can be attributed to

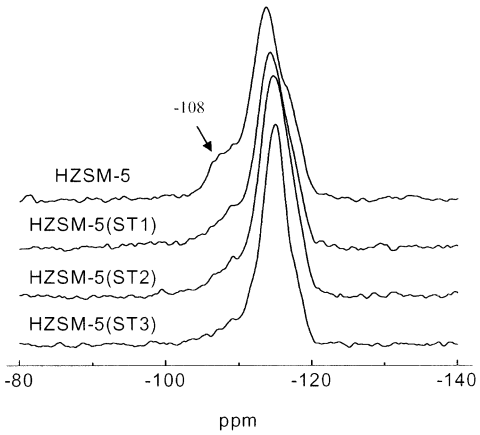

Figure 1. ^{29}Si MAS NMR spectra of parent HZSM-5 and those after steam treatment.

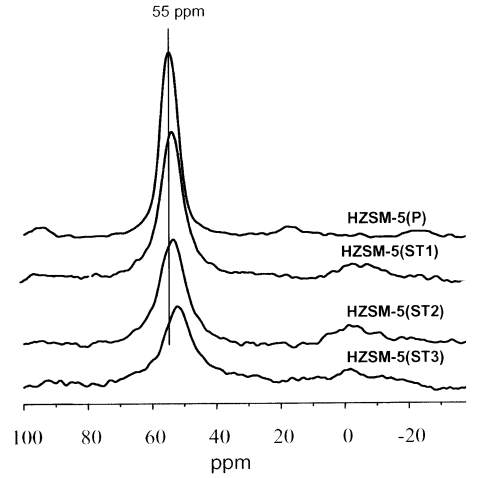

Figure 2. ^{27}Al MAS NMR spectra of parent HZSM-5 and those after steam treatment. Prior to the experiments, the samples were completed hydrated in a desiccator with saturated NH_4NO_3.

the crystallographically inequivalent Si(0Al) sites, while the one at −108 ppm is attributed to Si(1Al) species.[21] The silanol group ($(OSi)_3SiOH$) normally appears at −103 ppm, which is barely visible in the spectrum of parent HZSM-5. For HZSM-5(ST1), the intensity of peak at −108 ppm decreased, which suggests that part of the framework aluminum is removed from the zeolite lattice during steam treatment. By increasing the severity of the treatment (through an increase of the temperature or the partial pressure of the treatment), the intensity of the peak at −108 ppm decreased steadily (Figure 1, for top to bottom). In the case of HZSM-5(ST-3), only a small amount of such species remained (less than one-sixth of that of the parent zeolite). Present observations suggest that the removal of framework aluminum from the zeolite can be controlled by the steaming temperature, the partial pressure of steam, and the duration of the steaming. The more harsh the condition applied, the more severe the dealumination observed.

^{27}Al MAS NMR experiments provide more valuable information regarding the steam dealumination of the zeolite. As shown in Figure 2, the parent HZSM-5 shows a single line at 55 ppm, the origin of which is the tetrahedral aluminum species within the zeolite framework, while no signal of nonframework aluminum is detected, demonstrating that all the aluminum is in a tetrahedral coordination. Upon steam treatment, it is obvious that a new signal at 0 ppm appears, which is attributed to the expelled framework aluminum that forms nonframework octahedral aluminum that is probably in the form of $[Al(OH)_n]^{3-n}$ and $Al(H_2O)_6^{3+}$, etc.[22] At the same time, steam treatment broadens the main peak at ∼55 ppm and lowers its intensity. The total intensity of the aluminum signals of the treated samples decreased when compared with the parent HZSM-5. Moreover, it is interesting to note that the peak maximum of this resonance gradually shifts to high field part (to around 52 ppm in the case of HZSM-5(ST3)) upon dealumination. These facts suggest that (1) some of the framework aluminum is extracted from the zeolite lattice, with part of these extracted aluminum being transformed to octahedral species and part of them becoming NMR-invisible due to their lower symmetry, and (2) some of the aluminum retains the tetrahedral geometry, but the coordination environment of these aluminum are heavily distorted and thus leads to the observed line broadening. The peak maximum shift after steaming treatment is worthy of a further explanation, which will be discussed in the below section.

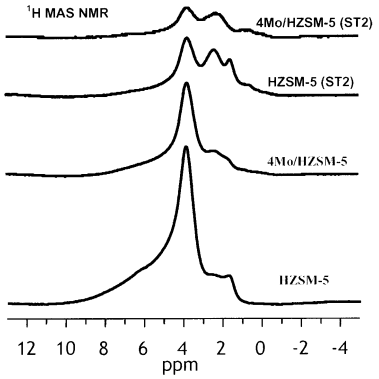

Figure 3. ^{1}H MAS NMR of HZSM-5(P) and HZSM-5(ST2) before and after molybdenum loading.

^{1}H MAS NMR spectra of parent HZSM-5 and HZSM-5(ST2) are shown in Figure 3. Four peaks at 1.7, 2.2, 4.0, and 6.2 ppm from the parent zeolite can be clearly resolved. The 1.7 and 2.2 ppm peaks are attributed to silanol group and Al−OH species, respectively.[23] The peak at 4.0 ppm is bridging OH groups (Brönsted acid sites), while the resonance at 6.2 ppm is commonly assigned to another kind of Brönsted acid site, which is influenced by the additional electrostatic interaction of the zeolite framework.[23] While the silonal group and Al−OH species are kept almost intact after steam treatment (the amount of Al−OH increases slightly due to the formation of nonframework aluminum, as described above), the amount of the two Bronsted sites decreases dramatically; i.e., about 70% Bronsted acid sites are removed with respect to the parent HZSM-5, showing the efficiency of steam dealumination. It is well-known that Bronsted acid sites could be described as framework bridging hydroxyl groups, i.e. $Si-OH-Al(OSi)_3$ species with the aluminum being in a framework tetrahedral geometry.[24] With this in mind, it is interesting to note that the present observation from proton NMR seems to be in conflict with the ^{27}Al MAS NMR result: in the ^{27}Al MAS NMR of HZSM-5(ST2), only about 30−40% of the tetrahedral framework aluminum (at around 55 ppm) is removed as compared with that of the parent zeolite. Meanwhile, one should notice that the ^{29}Si MAS NMR that is shown previously (Figure 1) also supports the proton NMR result. The intensity of the line corresponding to the Si(1Al) groups lost around 60% after being dealuminated under 823 K, 38 kPa for 6 h. Thus, it is worthwhile to reconsider the assignment of the peak at around 55 ppm in the ^{27}Al MAS NMR spectra. It is demonstrated by Klinowski et al.[25] that by using quadrupole nutation experiments, both Al^F and Al^{NF} are suggested to be the sources for the formation of the tetrahedral Al species). Through the observation of the structural changes

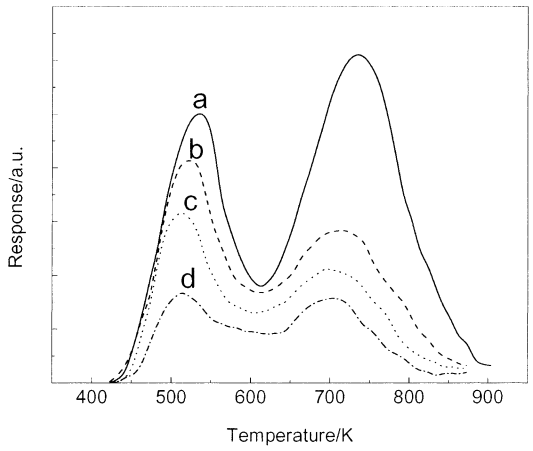

Figure 4. NH_3-TPD profiles of (a) HZSM-5(P), (b) HZSM-5(ST1), (c) HZSM-5(ST2), and (d) HZSM-5(ST3).

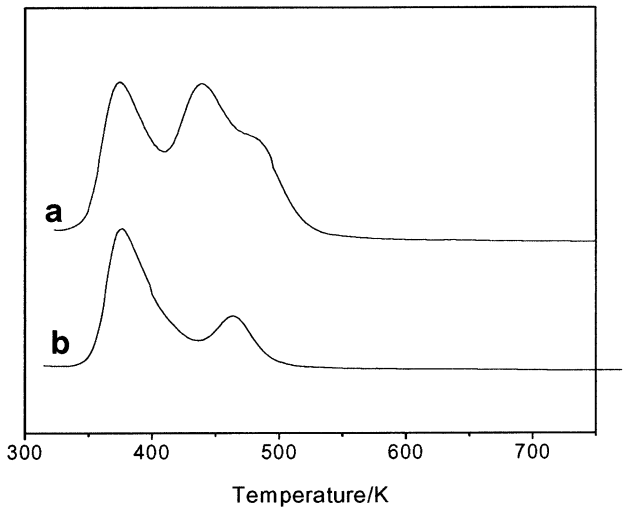

Figure 5. Benzene-TPD profile of HZSM-5(P) and HZSM-5(ST2).

of a series of hydrothermally dealuminated HZSM-5 samples, Long et al. concluded that a new tetrahedral aluminum species (around 55 ppm) is formed during the formation of nonframework octahedral aluminum species after a heavy dealumination treatment.[26] This species was proven not to be staying within the zeolite framework but a kind of nonframework tetrahedral Si−O−Al species that probably adheres to the surface of the zeolite. Recently, we have also reported that tetrahedral nonframework Al is formed after a steam treatment on HMCM-22.[27] As compared with the tetrahedral framework aluminum species, it has shifted to the high field part in the ^{27}Al MAS NMR spectrum. Therefore, it is reasonable to ascribe the observed 52 ppm peak to the overlap of both the framework and nonframework tetrahedral aluminum species. Only the framework tetrahedral aluminum species contribute to the Bronsted acidic sites, which releases Bronsted H when participating in the proton-transfer or aromatization reactions.[28]

NH_3-TPD can give out the information not only about the amount of the acid sites but also about alternation of the acid strength distribution. Figure 4 shows the NH_3-TPD profiles of HZSM-5 before and after steaming treatments. There are two peaks centered at 530 and 740 K, respectively. The former can be assigned to the desorption peak of physisorbed ammonia or ammonia adsorbed on the weak acid sites, while the high-temperature desorption peak is the strong acid site that is Bronsted in nature.[13] With the steam treatment, it is apparent that the amount of ammonia adsorbed on the Bronsted acid site dropped sharply, which confirms the ^{29}Si and ^{1}H MAS NMR results. Meanwhile, the acid strength is modified: after hydrothermal dealumination at 773 K and 38 kPa for 6h, the peak center of the high-temperature peak shifts from 740 to 710 K (Figure 4a,b). It further decreases to about 700 K when applying a more rigorous treatment condition (Figure 4c,d). Thus, both the amount and the strength of the acid sites are modified through the hydrothermal dealumination.

Some authors have suggested that in the hydrothermal treatment, the medium acid strength sites were removed, and only a fraction of the strongly acidic center was preserved.[29,30] At the same time, it is concluded that as the initial framework aluminum starts to decrease, the fraction of isolated Al atoms increases, thus resulting in an increase in the acid strength of the active sites. The authors attributed the observed enhanced catalytic activity of the dealuminated zeolite in some reaction to the formation of the very strong acid sites upon dealumination. However, based on the present NH_3-TPD result, we did not observe the existence of the very strong acid cites caused by the formation of isolated Al atoms. On the other hand, it is obvious that the aluminum atoms associated with strong Bronsted sites are expelled from the lattice after steam treatment. By FT-IR, NH_3-stepwise temperature programmed desorption, Simrniotis et al. reported that for high siliceous zeolite like ZSM-12, an increase of the dealumination severity results in a decrease of acid site strength.[31−33] This conclusion was also confirmed by Masuda et al. in case of HZSM-5.[34] As is well-known, benzene is the main product of the methane aromatization reaction. So, it is of special interest to use benzene as a probe to detect the acidity of these samples. Benzene-TPD profiles of parent HZSM-5 and HZSM-5(ST2) are shown in Figure 5. It is obvious that the low peak at 380 K that can be attributed to physisorbed benzene did not alter much after dealumination, while the two high-temperature peaks (at 460 and 490 K), which can be attributed to the benzene that absorbed on the Bronsted acid sites, shrink sharply after dealumination. This strongly suggests that the amount and the strength of acid sites that are available for benzene adsorption are heavily modified upon steam treatment.

3.2. Catalysts Evaluation. From the above discussion, it is clear that framework tetrahedral aluminum species associated with the strong Bronsted acid sites are preferentially removed from the zeolite lattice during the steaming treatment. In the following section, the effects of the removal of these sites in methane aromatization reaction are illustrated.

Figure 6 shows the methane conversion, benzene yield, and the distribution of various products of Mo/HZSM-5 and Mo/HZSM-5(STn) after 360 min of stream at 973 K and 1 atm. While methane conversion of heavily dealuminated catalyst Mo/HZSM-5(ST3) dropped sharply to less than 6% due to a loss in lattice crystallinity (about 60% of that of the parent, XRD pattern not shown here), it is clear that CH_4 remained almost stable (about 9.5%) for the Mo/HZSM-5(P), Mo/HZSM-5(ST1) and Mo/HZSM-5(ST2) catalysts (Figure 6a). On the contrary, a dramatic increase of benzene yield is observed after steam treatment. Compared with Mo/HZSM-5(P), the benzene yield of dealuminated catalysts gradually reaches a plateau at Mo/HZSM-5(ST2), raised by about 1/3, i.e., from 4.8% to 6.4%. With methane conversion being similar, an increase in benzene yield means that the product distribution of this reaction changed. It is interesting to note that the enhancement of benzene selectivity after dealumination treatment comes from the strong suppression of coke formation (the selectivity toward toluene and naphthalene almost remains constant; see Figure 6b). For

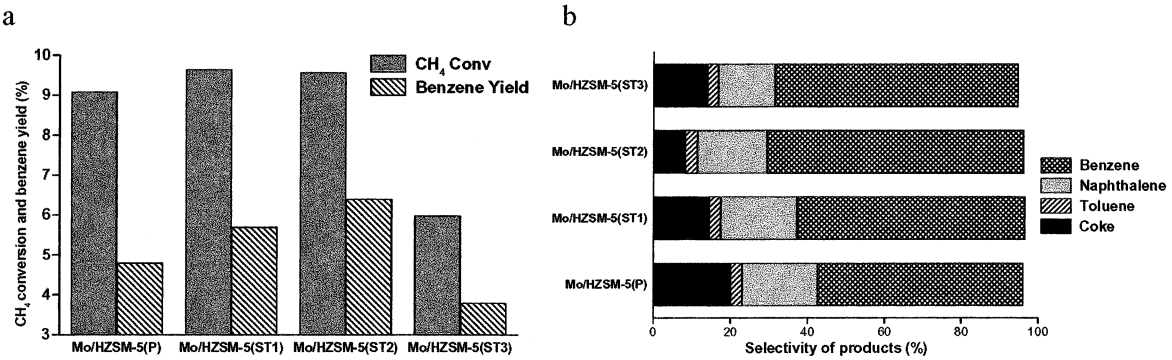

Figure 6. Methane conversion, benzene yield (a), and products distribution (b) of Mo/HZSM-5(P) and Mo/HZSM-5(STn) ($n = 1-3$) catalysts after 360 min time-on-stream of methane aromatization reaction (973 K, 1 atm, GHSV = 600 h^{-1}).

TABLE 1: Catalytic Performance of 4 wt % Mo/HZSM-5(P), 4 wt % Mo/HZSM-5(HCl), and 4 wt % Mo/HZSM-5(ST2) Catalysts[a]

catalyst (4 wt %)	methane conversion/%	selectivity/% benzene	toluene	naphthalene	C_2^{2-}	C_2^0	coke	yields of aromatics/%
Mo/HZSM-5(P)	11.9	46.1	2.7	6.3	4.7	1.1	37.9	6.6
Mo/HZSM-5(HCl)	11.7	48.6	2.2	7.0	4.3	1.6	35.2	6.8
Mo/HZSM-5(ST2)	10.9	63.5	3.1	8.3	4.9	1.4	18.9	8.7

[a] Time-on-stream, 420 min; reaction temperature, 1023 K; reaction pressure, 1 atm; GHSV, 600 h^{-1}.

the parent and HZSM-5 supported molybdenum catalysts dealuminated to different extents, the coke selectivity bottomed out at Mo/HZSM-5(ST2) (for Mo/HZSM-5(P), it is 20.3%, while that of Mo/HZSM-5(ST2) is 8.2%), in line with the maximum of benzene selectivity. Parallel improved catalytic behaviors are obtained as for the reaction conducted at 1023 K (Table 1), where the yields of aromatics on dealuminated catalyst after 420 min on stream is about 32% higher than that of parent Mo/HZSM-5(P) (8.7% via 6.6%). These facts are inevitably related to the modification of acidity by steam treatment. As shown in the above section, steam treatment leads to the removal of the tetrahedral framework aluminum, which is associated with the Bronsted acidity of the zeolite. At the same time, it is shown by the NH_3-TPD that it is the strongest acid sites that are removed during the steaming process, thus resulting in a decrease in both the amounts and the strength of the Bronsted acid sites. Coupling with current catalyst evaluation results, it can be concluded that only a small fraction of Bronsted sites are useful for reaction. Considering that the amount of Bronsted acid sites will further decrease after loading of molybdenum (see Figure 3), what is beyond our imagination is that although only less than 15% of the Bronsted acid sites of the parent zeolite remain after steaming at 823 K, 38 kPa for 6 h, these acid sites are already sufficient to accomplish the aromatization process of intermediates in the methane aromatization reaction! At the same time, these unnecessary Bronsted sites just promote the carbonaceous deposition of this reaction, which agrees very well with the conclusions of Smirnoitis et al.:[33] too many very strong acid sites may result in (1) the holding of coking precursors for a longer time on the surface, which allows for further polymerization reactions of these precursors, and (2) higher activity for coking reaction. The increase and the growing of these carbonaceous species will eventually lead to a channel blockage of the zeolite, and as a result, the reactants are unable to gain access to the active sites while it is difficult for the product to diffuse out of the zeolite channel; therefore, a so-called "death" of the catalyst occurs. Figure 7 shows the aromatics yield of Mo/HZSM-5(P) and Mo/HZSM-5(ST2) catalysts with time-on-stream at 973 and 1023 K. For reaction under 973 K, it is clear that the deactivation of Mo/HZSM-5(P) is more pronounced

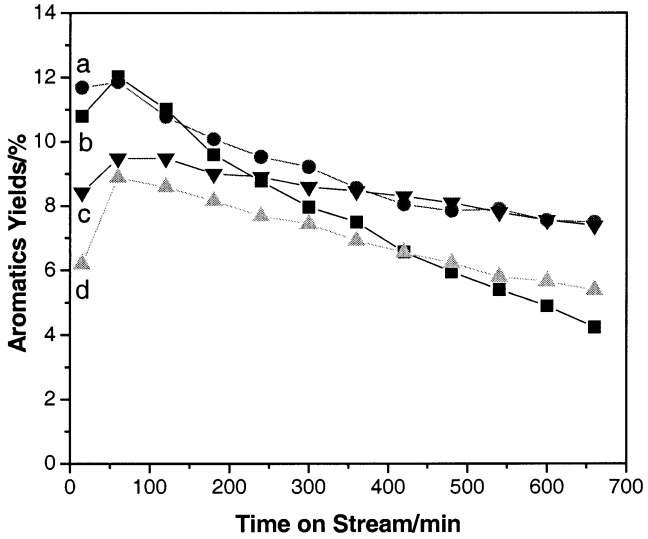

Figure 7. The aromatics yields of (a) Mo/HZSM-5(ST2) and (b) Mo/HZSM-5(P) catalysts with time-on-stream (1023 K; 1 atm; GHSV = 600 h^{-1}); (c) Mo/HZSM-5(ST2) and (d) Mo/HZSM-5(P) catalysts with time-on-stream (973 K, 1 atm, GHSV = 600 h^{-1}).

than that of Mo/HZSM-5(ST2) (Figure 7c,d). Meanwhile, a higher reaction temperature will result in a heavier coke formation and thus a severe activity loss. One can notice that the deactivation of both these two catalysts is fast in the initial stage for the reaction under 1023 K (Figure 7a,b). While the aromatics yield of Mo/HZSM-5(ST2) catalyst stayed almost the same (around 8%) after 400 min time-on-stream, that of the Mo/HZSM-5(P) significantly dropped with further reaction.

The present investigation demonstrated that only a small fraction of Bronsted sites, which have a relatively weak acid strength when compared with the parent HZSM-5, is necessary for Mo/HZSM-5 to be an efficient and effective methane aromatization catalyst. Superfluous Bronsted acid sites, especially those with strong acid strength, would benefit the formation of aromatic-type coke species, which may initiate and grow in these sites and then ultimately lead to the channel blockage and the death of the catalysts. It is just the removal of

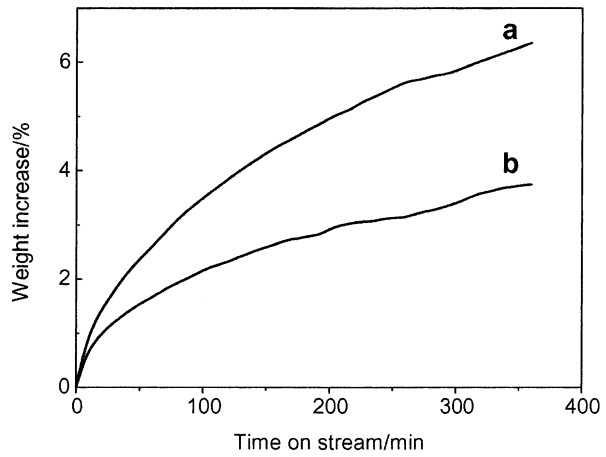

Figure 8. In situ TG profiles of (a) Mo/HZSM-5(P) and (b) Mo/HZSM-5(ST2) catalysts with time-on-stream. Similar conditions as those in a real fixed-bed reaction (973 K, 1 atm, GHSV = 600 h^{-1}) were used.

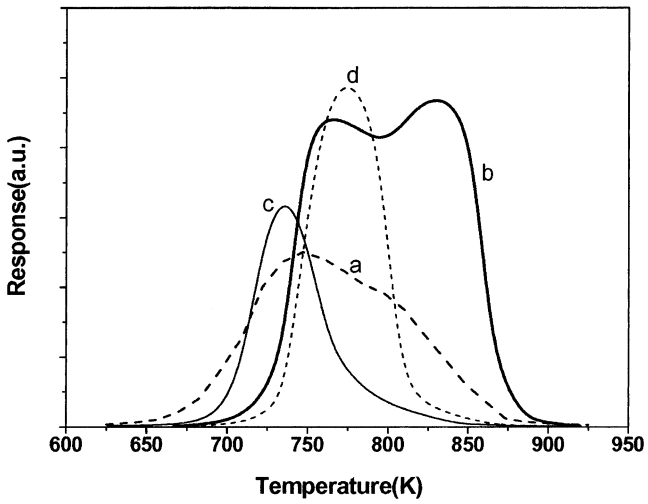

Figure 9. TPO profiles of (a) Mo/HZSM-5(P) after reaction at 973 K for 8 h; (b) Mo/HZSM-5(P) after reaction at 1023 K for 8 h; (c) Mo/HZSM-5(ST2) after reaction at 973 K for 8 h; (d) Mo/HZSM-5(ST2) after reaction at 1023 K for 8 h. All the methane aromatization reactions were conducted at 1 atm, GHSV = 600 h^{-1}.

excess framework aluminum that inhibits the formation of these harmful cokes and therefore increases the benzene yield and durability of catalysts.

3.3. Carbonaceous Deposits on the Catalysts. Figure 8 shows the in situ TG profiles of Mo/HZSM-5(P) and Mo/HZSM-5(ST2) catalysts with time-on-stream. A condition is selected to simulate the real fixed-bed reaction. Two kinds of slopes can be found in the TG profiles: the weight increase speeds are very fast before 20 min time-on-stream, while they gradually slow with further reaction. The weight increase speeds of these two catalysts are similar in the initial stage of the reaction (<20 min). As shown in TPSR, the reaction before about 20 min is the so-called induction period of this reaction,[35] and a transformation of molybdenum oxide to molybdenum carbide is dominant for this period, which is so violent that to a certain degree it is just like a phase transfer reaction. With further reaction, benzene formation is observed and the aromatic-type carbonaceous deposits on the Bronsted sites are the result.[35] At the same time, carbonaceous deposits associated with molybdenum continue to increase at this stage. It is obvious that the TPO profiles (Figure 9) of deactivated Mo/HZSM-5(P) catalyst (after 8 h reaction at 973 and 1023 K, respectively) are

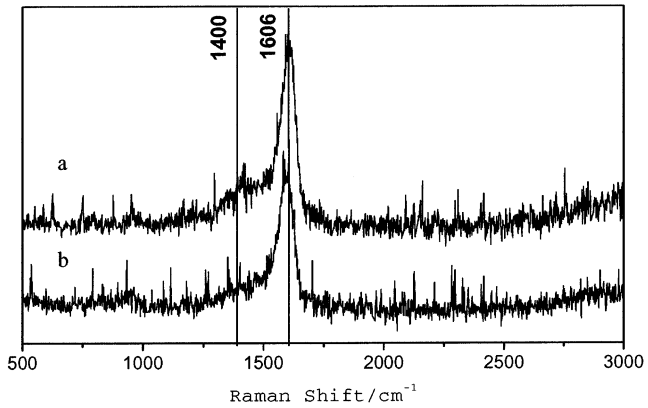

Figure 10. UV−Raman spectra of (a) Mo/HZSM-5(P) and (b) Mo/HZSM-5(ST2) catalysts after reaction at 973 K for 6 h (1 atm, GHSV = 600 h^{-1}).

of a double-peak structure, with the low-temperature oxidation peak attributed to carbon associated with molybdenum, whereas the high-temperature peak is assigned to carbonaceous deposit on zeolite Bronsted acid sites.[35,36] After pre-dealumination treatment (TPO profiles of coked Mo/HZSM-5(ST2)), the amount of coke on the catalysts remarkably decreased. In fact, only a peak that is the low temperature peak of TPO of coked Mo/HZSM-5(P) could be monitored, in conjunction with an indistinctive tail in high-temperature region. This observation properly supports our conclusion that dealumination can successfully remove the excessive framework aluminum (Bronsted sites) and thus overcome the main drawback of this reaction, acid-associated carbonaceous depositions in the methane aromatization reaction. A variation of the TG curve of these two catalysts after the induction period agrees very well with the TPO results: the Mo/HZSM-5(P) catalyst presents a higher coke formation speed as compared with the dealuminated Mo/HZSM-5(ST2) catalyst (Figure 8). The reason for the observed difference is that the amounts of molybdenum-associated coke on these two catalysts are similar during the reaction (>20 min), while the aromatic-type coke on acid sites is heavily suppressed in the case of Mo/HZSM-5(ST2) with respect to the Mo/HZSM-5(P) catalyst.

To further confirm the coke-suppress effect caused by the steam treatment, UV−Raman spectroscopy[37] was used to study the deactivated catalysts after 6 h of stream at 973 K (Figure 10). Both the deactivated Mo/HZSM-5(P) and Mo/HZSM-5(ST2) catalysts give out signals at 1300−1700 cm^{-1}, while no band at about 3000 cm^{-1} is observed, indicating that these cokes are not a hydrogen-rich paraffinic coke species. In the case of Mo/HZSM-5(P), a band at 1606 cm^{-1} appears with a broad shoulder at about 1400 cm^{-1}, both of which come from the coke species.[38] The 1606 cm^{-1} band seems to be composed of several components. It is due to the C=C stretching mode, which resulted from the polyaromatic, substituted aromatic or even graphite species, depending on the different wavenumbers. A lower wavenumber always indicates lower hydrogen content in the corresponding coke species.[37] The shoulder at about 1400 cm^{-1} is assigned to the C−H bending mode of the coke species. For the UV−Raman spectrum of deactivated Mo/HZSM-5(ST2) catalyst, it is apparent that the main band at around 1606 cm^{-1} shifts to 1585 cm^{-1}, whereas the broad band at 1400 cm^{-1} almost disappears. This fact (band shift, etc.) suggests that the formation of the polyaromatic and substituted aromatic species are suppressed for the catalyst with less Bronsted acid sites,

while the graphite or quasi-graphite species associated with molybdenum remains. This is in agreement with the above TPO results.

4. Conclusions

A remarkable improvement on the catalytic performance of Mo/HZSM-5 catalysts for methane aromatization reaction is reached by steam-treating the support, HZSM-5. A proper steam treatment leads to the removal of part of the tetrahedral framework aluminum from the zeolite lattice and thus to the reduction of both the amount and the strength of Bronsted acid sites of the catalyst. While these superfluous Bronsted acid sites are proven to be useless for the intermediate aromatization of methane aromatization reaction, they actually facilitated the holding of coking precursors for a longer time on the surface, which allows for the further polymerization reactions of these precursors, thus largely increasing the aromatic-type carbonaceous deposition. Removal of these unnecessary Bronsted acid sites by steam treatment leads to an efficient and effective suppression of the aromatic coke in the current reaction. Therefore, a much higher benzene yield and a longer durability of the catalysts are obtained when compared with the conventional Mo/HZSM-5 catalysts.

Acknowledgment. We are very grateful for the support of the National Natural Science Foundation of China and the Ministry of Science and Technology of China and to Prof. Can Li and Mrs. Jian Li for their kind help in the UV−Raman experiments.

References and Notes

(1) Crabtree, R H. *Chem. Rev.* **1995**, *95*, 987.
(2) Lunsford, J. H. *Catal. Today* **2000**, *63*, 165.
(3) Wolf, D. *Angew. Chem., Int. Ed.* **1998**, *37*, 3351.
(4) Axelrod, M. G.; Gaffney, A. M.; Pitchai, R.; Sofranko, J. A. In *Natural Gas Conversion II*, Curry-Hyde, H. E., Howe, R. F., Eds.; Elsevier: New York, 1994; P93.
(5) Labinger, J. A. *Stud. Surf. Sci. Catal*, **1997**, *136*, 325.
(6) Wang, L.; Tan, L.; Xie, M.; Xu, G.; Huang, J.; Xu, Y. *Catal. Lett.* **1993**, *21*, 35. Xu, Y.; Liu, S.; Wang, L.; Xie, M.; Guo, X. *Catal. Lett.* **1995**, *30*, 135.
(7) Wang, D.; Lunsford, J. H.; Rosynek, M. P. *Top. Catal.* **1996**, *3*, 289; Wang, D.; Rosynek, M. P.; Lunsford, J. H. *J. Catal.* **1997**, *169*, 347.
(8) Solymosi, F.; Erdöhelyi, A.; Szöke, A. *Catal. Lett.* **1995**, *32*, 43. Solymosi, F.; Szöke, A.; Cserényi, J. *Catal. Lett.* **1996**, *39*, 157; Solymosi, F.; Cserényi, J.; Szöke, A.; Bansagi, T.; Oszkó, A. *J. Catal.* **1997**, *165*, 150; Solymosi, F.; Bugyi. L.; Oszkó, A. *Catal. Lett.* **1999**, *57*, 103.
(9) Zhang, J. Z.; Long, M. A.; Howe, R. F. *Catal. Today* **1998**, *44*, 293.
(10) Borry, R. W., III; Kim, Y. H.; Huffsmith, A.; Reimer, A.; Iglesia, I. *J. Phys. Chem. B* **1999**, *103*, 5787; Kim, Y.; Borry, R. W., III; Iglesia, E.; *Microporous Mesoporous Mater.* **2000**, *35*−*36*, 495.
(11) Liu, S.; Dong, Q.; Ohnishi, R.; Ichikawa, M. *Chem. Commun.* **1998**, 1217; Liu, S.; Wang, L.; Ohnishi, R.; Ichikawa, M.; *J. Catal.* **1999**, *181*, 175.
(12) Bouchy, C.; Schmidt, I.; Anderson, J. R.; Jacobsen, C. J. H.; Derouane, E. G.; Derouane-Abd Hamid, S. B. *J. Mol. Catal. A* **2000**, *163*, 283; Derouane-Abd Hamid, S. B.; Anderson, J. R.; Schmidt, I.; Jacobsen, C. J. H.; Derouane, E. G. *Catal. Today* **2000**, *63*, 461.
(13) Ma, D.; Shu, Y.; Bao, X.; Xu, Y.; *J. Catal.* **2000**, *189*, 314; Ma, D.; Zhang, W.; Shu, Y.; Xu, Y.; Bao, X. *Catal. Lett.* **2000**, *66*, 155.
(14) Lu, Y.; Xu, Z.; Tian, Z.; Zhang T.; Lin, L. *Catal. Lett.* **1999**, *62*, 215.
(15) Liu, S.; Dong, Q.; Ohnishi, R.; Ichikawa, M. *Chem. Commun.* **1999**, 1455.
(16) Ohnishi, R.; Liu, S.; Dong, Q.; Wang, L.; Ichikawa, M. *J. Catal.* **1999**, *182*, 92.
(17) Yuan, S.; Li, J.; Hao, Z.; Feng, Z.; Xin, Q.; Ying, P.; Li, C. *Catal. Lett.* **1999**, *63*, 73.
(18) Campbell, S. M.; Bibby, D. M.; Coddington, J. M.; Howe, R. F. *J. Catal***. 1996**, *161*, 350.
(19) Sahoo, S. K.; Viswanadhanm, N.; Ray, N.; Gupta, J. K.; Singh, I. D. *Appl. Catal. A: General* **2001**, *205*, 1.
(20) Lu, Y.; Ma, D.; Xu, Z.; Tian, Z.; Bao, X.; Lin, L. *Chem. Commun.* **2001**, 2048.
(21) Campbell, S. M.; Bibby, D. M.; Coddington, J. M.; Howe, R. F.; Meinhold, R. H. *J. Catal.* **1996**, *161*, 338.
(22) Ma, D.; Deng, F.; Fu, R.; Han, X.; Bao, X. *J. Phys. Chem B* **2001**, *1055*, 1770.
(23) Hunger, M. *Catal. Rev.-Sci. Eng.* **1997**, *39*, 345.
(24) Hagg, W. O.; Lago, R. M.; Weisz, P. B. *Nature* **1984**, *309*, 1984;
(25) Rocha, J.; Carr, S. E.; Klinowski, J. *Chem. Phys. Lett.* **1991**, *187*, 401.
(26) Long, Y.-C.; Jin, M.-Y.; Sun, Y.-J.; Wu, T.-L.; Wang, L.-P.; Fei, L. *J. Chem. Soc., Faraday Trans.* **1996**, *92*, 1647.
(27) Ma, D.; Han, X.; Bao, X.; Hu, H.; Au−Yeung, S. C. F. *Chem. Eur. J.* **2002**, *8*, 162.
(28) Ma, D.; Shu Y.; Zhang, W.; Han, W.; Xu, Y.; Bao, X. *Angew. Chem., Int. Ed. Engl.* **2000**, *39*, 2928.
(29) Mishin, I. V.; Pal-Borbely, G.; Karge, H. G. *Stud. Surf. Sci. Catal.* **1995**, *94*, 294.
(30) Mishin, I. V.; Beyer, H. K.; Karge, H. G. *Appl. Catal. A: Gen.* **1999**, *180*, 207.
(31) Zhang, W.; Smirniotis, P. G. *Appl. Catal. A: Gen.* **1998**, *168*, 113.
(32) Zhang, W.; Burckle, E. C.; Smirniotis, P. G. *Microporous Mesoporous Mater.* **1999**, *33*, 173.
(33) Zhang, W.; Smirniotis, P. G. *Catal. Lett.* **1999**, *60*, 223.
(34) Masuda, T.; Fujikata, Y.; Mukai, S. R.; Hashimoto, K. *Appl. Catal. A: Gen.* **1998**, *172*, 73.
(35) Ma, D.; Shu Y.; Cheng, M.; Xu, Y.; Bao, X. *J. Catal.* **2000**, *194*, 105; Ma, D.; Wang, D.; Su, L.; Xu, Y.; Bao, X. *J. Catal.* In press.
(36) Lerner, B. A.; Zhang, Z.; Sachtler, W. M. H. *J. Chem. Soc. Fraday Trans.* **1993**, *89*, 1799.
(37) Li, C.; Stair, P. C. *Stud. Surf. Sci. Catal* **1997**, *105*, 599. and references therein.
(38) Colthup, N. B.; Fateley, W. G. et al. The Handbook of Infrared and Raman Characteristic Frequencies of Organic Molecules Academic Press: Boston, 1991.